27 Johnston, S, Manchester, R N, Lyne, A G, Nicastro, L. and Sprromilio, J, Mon Not R Astron Soc, 1994, **268**, 430–436
28 Manchester, R N and Johnston, S, *Astrophys J*, 1995, **441**, L65–L68
29 Watson, M and Bailes, M, unpublished, 1992.
30 Cominsky, L, Roberts, M and Johnston, S, *Astrophys J.*, 1994, **427**, 978–983
31 Greiner, J, Tavani, M and Belloni, T, *Astrophys J.*, 1995, **441**, L43
32 Kochanek, C S, *Astrophys J*, 1993, **406**, 638–650
33 King, A and Cominsky, L, *Astrophys J*, 1994, **435**, 411–415
34 Lipunov, V M, Nazin, S N, Osminkin, E. Y. and Prokhorov, M E, *Astr Astrophys*, 1994, **282**, 61–72.
35 Tavani, M, Arons, J and Kaspi, V. M, *Astrophys J.*, 1994, **433**, L37–L40
36 Manchester, R N, Johnston, S, Lyne, A G., D'Amico, N., Bailes, M and Nicastro, N, *Astrophys J*, 1995, **445**, L137.
37 Illarionov, A. F. and Sunyaev, R A., *Astr. Astrophys*, 1975, **39**, 185–195
38 Ghosh, P and Lamb, F K, *Astrophys J*, 1979, **234**, 296–316
39 Ghosh, P, *Astrophys J*, 1995 (in press)
40 Johnston, S, Manchester, R. N, Lyne, A. G, D'Amico, N, Bailes, M, Gaensler, B. M and Nicastro, L *Mon Not. R Astron Soc*, 1995 (submitted).
41. Melatos, A., Johnston, S and Melrose, D B, *Mon Not R Astron Soc*, 1995, **275**, 381–397.
42 Dougherty, S M, Waters, L. B F, Burki, G., Coté, J, Cramer, N, van Kerkwijk, M H and Taylor, A. R, *Astr Astrophys*, 1994, **290**, 609–622
43 Kaspi, V M, Tavani, M, Nagase, F., Hirayama, M, Hoshino, M, Aoki, T., Kawai, N. and Arons, J, *Astrophys J*, 1995 (submitted)
44. Tavani, M. and Arons, J, *Astrophys J*, 1995 (in preparation)
45. Grove, J. E., Tavani, M, Purcell, W R., Johnson, W. N, Kurfess, J D, Strickman, M S and Arons, J, *Astrophys. J*, 1995, **447**, L113–L15
46 McCollum, B, Castelaz, M W. and Bruhweiler, F. C., *Astrophys J*, 1995 (in preparation).
47. Unger, S. J and Johnston, S. *Mon. Not. R Astron Soc*, 1995 (in preparation)
48 Johnston, S, *et al*, *Mon Not R Astron Soc*, 1995 (in preparation)

Received 3 July 1995; revised accepted 12 July 1995.

A high-precision technique using X-ray reflectivity for the measurement of surface and interface roughness

P. V. Satyam, D. Bahr*, S. K. Ghose, G. Kuri, B. Sundaravel, B. Rout and B. N. Dev

Institute of Physics, Sachivalaya Marg, Bhubaneswar 751 005, India
*Hamburg Synchrotron Radiation Laboratory, HASYLAB at DESY, Notkestr. 85, D-22603 Hamburg, Germany

Surface and interface roughness plays a crucial role in ultrathin two-dimensional layers. We have set up an X-ray reflectometry facility for the measurement of surface and interface roughness with a precision better than 1 Å. As ion implantation is one of the techniques to fabricate ultrathin buried epitaxial layers, we have explored the effect of MeV ion implantation on surface roughness in two cases: Au-implanted $LiNbO_3$(001) and Co-implanted Si(111) samples. In both cases we have observed an implantation-induced enhancement of surface roughness. In addition, for the Co-implanted samples, we found unexpected interference fringes with dose-dependent periodicity.

HIGH-quality thin films are necessary for the fabrication of lower-dimensional structures for fundamental studies and for device fabrication in microelectronics. For the growth of high-quality films the role of solid–vacuum and solid–solid interfaces is very crucial. The quality of the thin film and the interfaces should be as good as possible. Therefore, one needs experimental probes to determine this quality. Among the relevant questions to be answered are the following: (i) What is the structure of the ultrathin grown layer, or what is the initial stage of growth? (ii) For a multielemental film, which type of atoms lie in the first atomic layer at the interface? (iii) What is the coordination number of the interface atoms? (iv) What is the distance between adjacent atomic layers across the interface? These questions are answered by using a very powerful technique involving generation of standing waves of X-rays[1–4]. One would also like to know the amount of statistical disorder, or roughness, on the film surface and on the buried film–substrate interface. This information along with the film thickness can be obtained from X-ray specular reflectivity measurements. Both the X-ray standing wave and the X-ray reflectivity measurement techniques are nondestructive and the high penetration power of X-rays enables the probing of buried layers and interfaces.

For the determination of interface roughness, the problem is to determine the correct probability density function for the interface position in the direction of the surface normal. This is mostly a Gaussian distribution. Then the spread in the interface position can be evaluated. X-ray reflectivity under the grazing incidence condition is a well-established technique to investigate this spread in the position of exposed (outer) and buried (inner) interfaces[5].

We have recently set up the grazing incidence X-ray reflectivity experiment for the measurement of surface and interface roughness in the Institute of Physics, Bhubaneswar. To our knowledge, this is the first high-precision grazing incidence X-ray reflectometry facility in India. Here we present a brief description of the set-up and some preliminary results.

The experimental set-up uses an 18 kW rotating-anode X-ray source (RIGAKU 300VE) with a Mo anode. A line beam of Mo-$K_{\alpha 1}$ (17.479 keV) X-rays is selected with a symmetrically cut dislocation-free Si(111) monochromator crystal. The θ–2θ scan is performed using a HUBER four-circle diffractometer. The reflected X-rays are detected with a BaF_2 scintillation detector. The programs for the angular scans and data collection have been written in GWBASIC. A schematic diagram of the experimental set-up is shown in Figure 1. We also measure inelastic spectra, e.g. fluorescence, from the sample with a Si(Li) detector simultaneously with the reflectivity as a function of θ. The signal from the Si(Li), which first goes to a multichannel analyser, is automatically transferred to the computer (PC-386) memory along with the reflectivity data. The whole process is automated and controlled through the PC. This completes the set-up for X-ray standing wave experiment under grazing incidence specular reflection. This additional feature with the Si(Li) detector has not been shown in Figure 1. The details of the instrumentation aspect will be published elsewhere. A part of the instrumentation has already been published[6].

For X-rays the (real part of) index of refraction of any solid or liquid medium is less than unity. Thus, it is possible to obtain total external reflection from matter. For the two-media system the reflectivity is obtained from the Fresnel coefficient of reflection[5]:

$$r_{1,2} = \frac{k_{z,1} - k_{z,2}}{k_{z,1} + k_{z,2}}, \quad (1)$$

where

$$k_{z,l} \cong k_1(\theta_1^2 - 2\delta_l - 2i\beta_l)^{1/2}, \quad l = 1, 2, \quad (2)$$

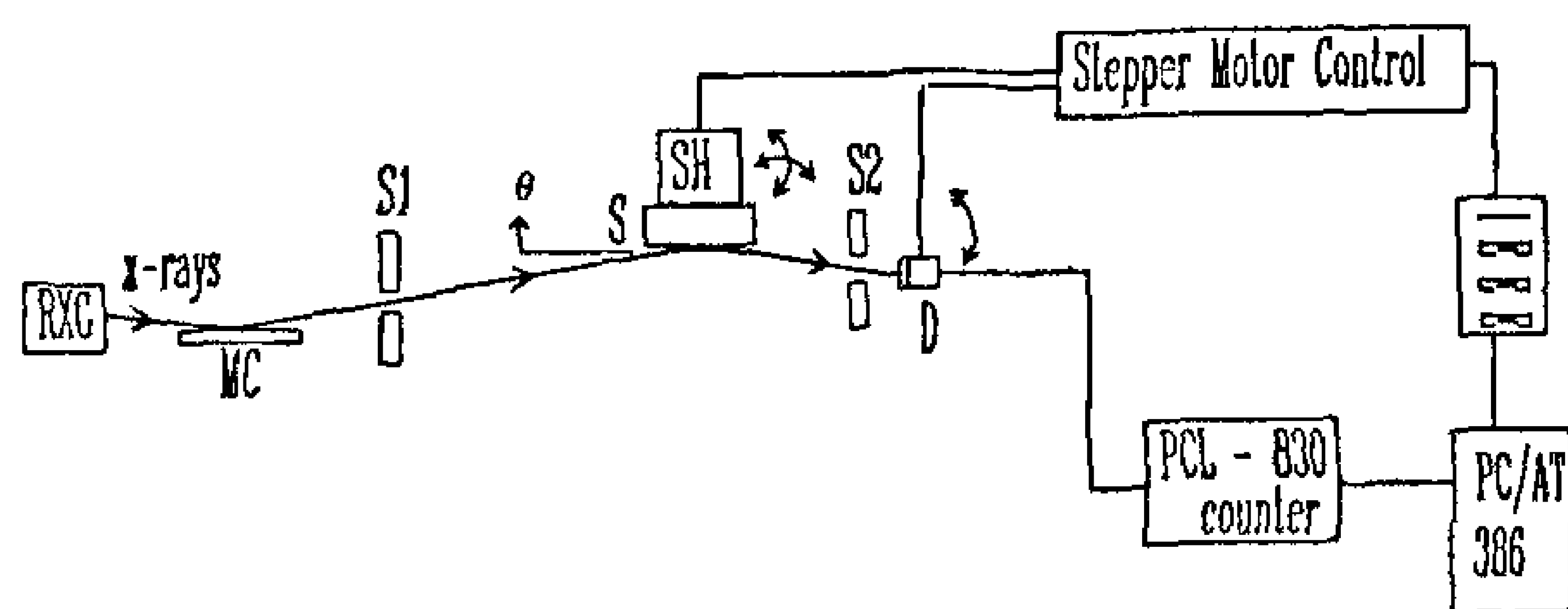

Figure 1 The schematic experimental set-up for X-ray reflectivity measurements

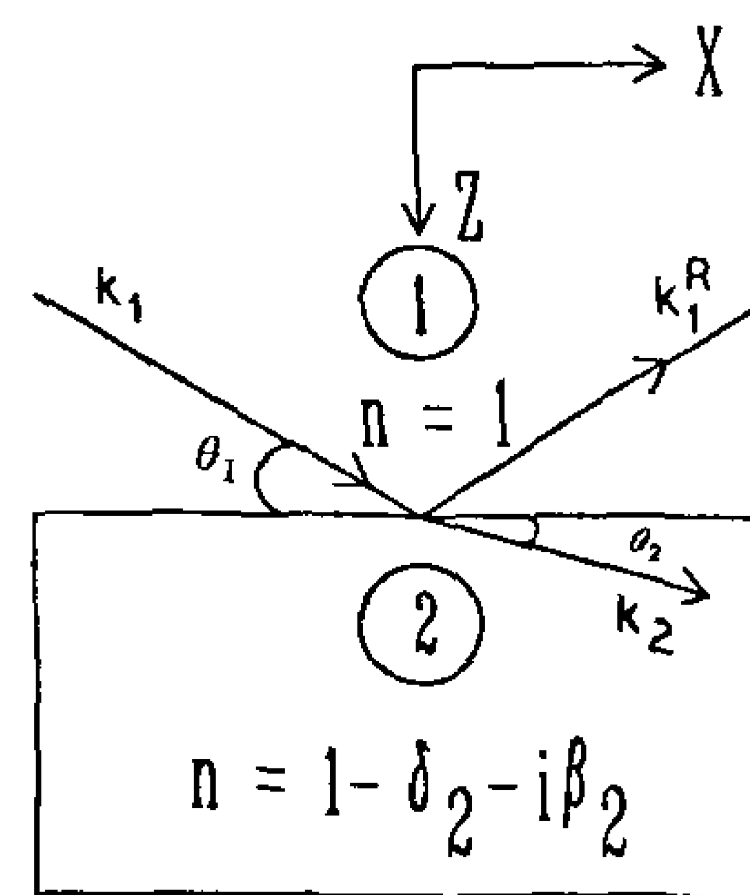

Figure 2 Sketch of X-ray reflection and refraction for a two-medium system

θ_1 and k_1 being the glancing angle and the wave vector in medium 1, respectively (Figure 2);

$$n_l = 1 - \delta_l - i\beta_l \quad (3)$$

is the complex refractive index of the material of the lth layer. δ and β values are very small, each of the order of 10^{-5} or less. δ and β values are given by $\delta = r_e \lambda^2 N/2\pi$ and $\beta = \lambda\mu/4\pi$, where r_e is the classical electron radius, λ is the wavelength of the incident radiation, N is the total number of electrons per unit volume and μ is the linear absorption coefficient[7]. Equation (1) is valid for the s-polarized radiation. For the p-polarized radiation

$$r_{1,2}^{p} = \frac{k_{z,1}/n_1^2 - k_{z,2}/n_2^2}{k_{z,1}/n_1^2 + k_{z,2}/n_2^2}. \quad (4)$$

However, for X-rays ($n_l \approx 1$) eq. (4) reduces to eq. (1).

If the first medium is air ($\delta = \beta = 0$) and the second a solid substrate, the reflectivity is

$$R_{1,2} = |r_{1,2}|^2 = \left|\frac{\theta - (\theta^2 - 2\delta_2 - 2i\beta_2)^{1/2}}{\theta + (\theta^2 - 2\delta_2 - 2i\beta_2)^{1/2}}\right|^2. \quad (5)$$

(We have dropped the subscript of θ_1.) This is applicable for a smooth surface. (A surface is also called an air–solid or vacuum–solid interface.)

For a rough surface, the surface position can be described by a Gaussian probability distribution as introduced by Nevot and Croce[8]:

$$P(z) = \frac{1}{\sqrt{2\pi}\sigma_2} e^{-z^2/2\sigma_2^2}. \quad (6)$$

With this modification the Fresnel coefficient of reflection for a rough surface becomes

$$r_{1,2}^{\text{rough}} = r_{1,2} \exp^{-2\sigma_2^2 k_{z,1} k_{z,2}} \quad (7)$$

in the limit $\sigma_2 k_{z,2} < 1$; σ_2 is the root mean square roughness of the surface of medium 2, and $r_{1,2}$ is given by eq. (1). This result was also obtained by Sinha *et al.*[9] in a different approach within the distorted-wave Born approximation (DWBA). Thus, the reflectivity (eq.(5)) gets modified for a rough surface:

$$R_{1,2}^{\rm rough} = \left| r_{1,2}^{\rm rough} \right|^2. \tag{8}$$

Here we present some results of reflectivity measurements on Au-implanted $LiNbO_3$(0 0 1) and Co-implanted Si(1 1 1) single-crystal substrates. $LiNbO_3$ is a widely used dielectric material for optical waveguides. The waveguiding properties are controlled by incorporating impurities, e.g., Ti, in the $LiNbO_3$ lattice. It is important to determine the impurity site in the lattice[10]. For the lattice location of Au in $LiNbO_3$ we performed X-ray standing wave and ion-channeling experiments. These results will be published elsewhere. Here we present the results of measurements of surface roughness of an implanted sample.

Interest in Co implantation in Si arises from the fact that it is possible to fabricate a buried epitaxial $CoSi_2$ layer in Si by ion implantation of Co followed by annealing. This process is known as ion beam synthesis (IBS). The IBS-prepared silicides have received much attention as their electrical transport properties are better than those prepared by the conventional ultrahigh vacuum procedure. A possible application of an IBS-fabricated Si/$CoSi_2$/Si heterostructure is as a metal base transistor[11]. Measurement and control of interface roughness in these structures are important. The results of surface roughness measurements on Co-implanted Si(1 1 1) samples are presented here and compared with those on the virgin Si(1 1 1) sample.

Figure 3 shows the X-ray specular reflectivity from a virgin (0 0 1)-oriented $LiNbO_3$ sample as a function of the grazing incidence angle. The curve fitted to the data corresponds to a surface roughness of 9.6 Å. In order to elucidate the precision of the roughness measurement, the theoretical curves for two values of roughness of 8.6 and 10.6 Å are also shown. These curves are clearly different from the best fit to the data, implying that the precision is better than 1 Å. The theoretical curves obtained from eq. (8) have been convoluted with the beam divergence (0.05°) for fitting to the experimental data. Results from the measurement on Au-implanted sample are shown in Figure 4, which also shows the virgin $LiNbO_3$ result for comparison. The measured roughness on the implanted sample is 14.5 Å, i.e. the surface roughness has been enhanced due to implantation. (It may be noted that high-energy ion implantation can produce interesting viscoelastic effect, leading to surface smoothing or roughening[12].) We have not made measurements on the implanted sample before annealing.

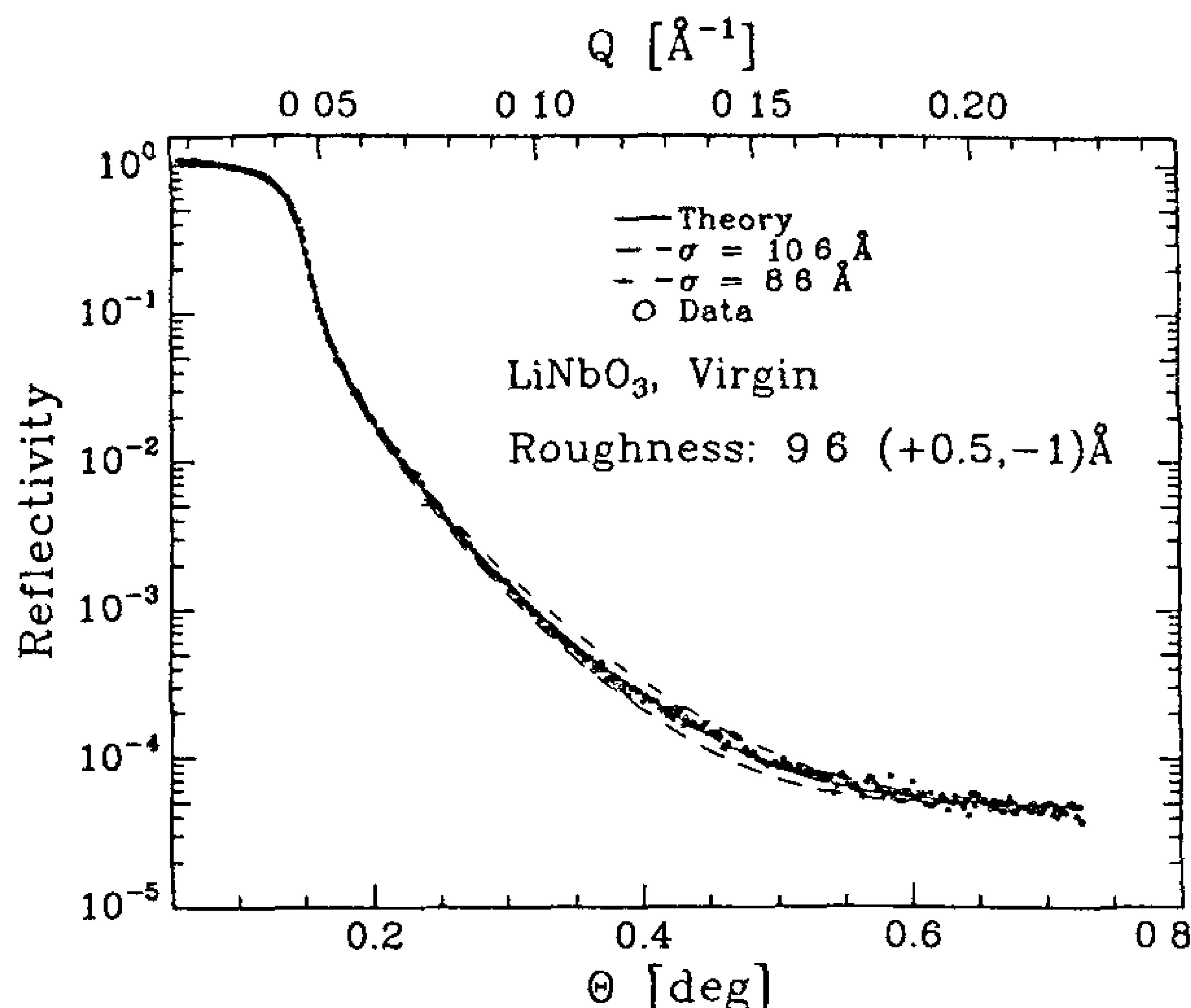

Figure 3 Reflectivity as a function of the grazing angle of incidence θ for a virgin $LiNbO_3$(0 0 1) sample. The value of the momentum transfer $Q = 4\pi \sin \theta/\lambda$ is shown on the top abscissa

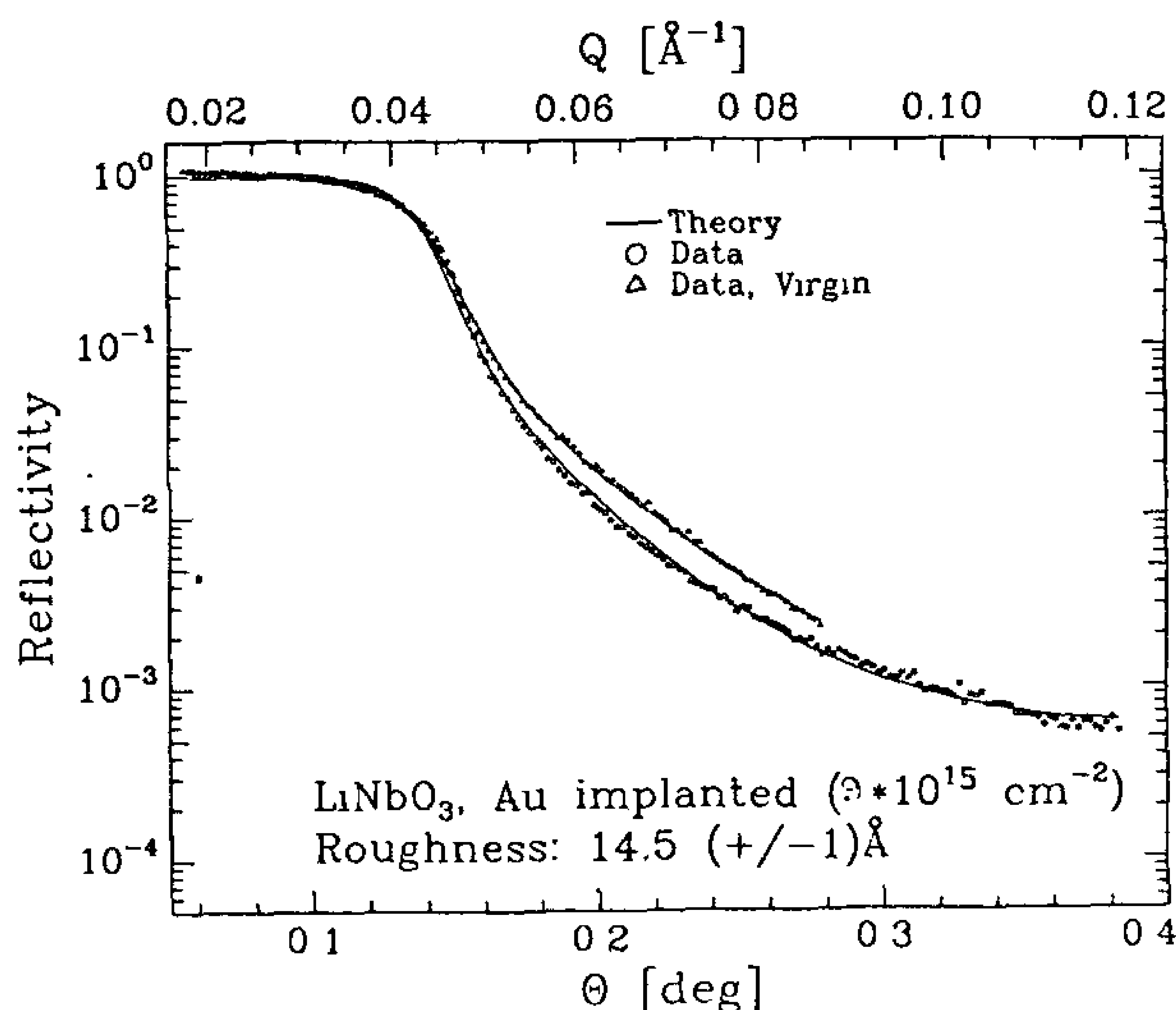

Figure 4 Reflectivity from an Au-implanted $LiNbO_3$(0 0 1) sample (O). For comparison the reflectivity from a virgin sample is also shown.

Surface roughness might have been even higher on the as-implanted sample. Au implantation was done using the 3 MV Pelletron accelerator in our Institute. 1.38 MeV Au^{2+} ions were implanted into the $LiNbO_3$ sample at a tilt angle (the angle between the surface normal and the ion beam direction) of 65°. The sample was annealed at 450°C for 40 min under flowing oxygen to remove implantation-induced lattice damage. The ion-channelling measurement showed that the bulk lattice damage was almost fully removed.

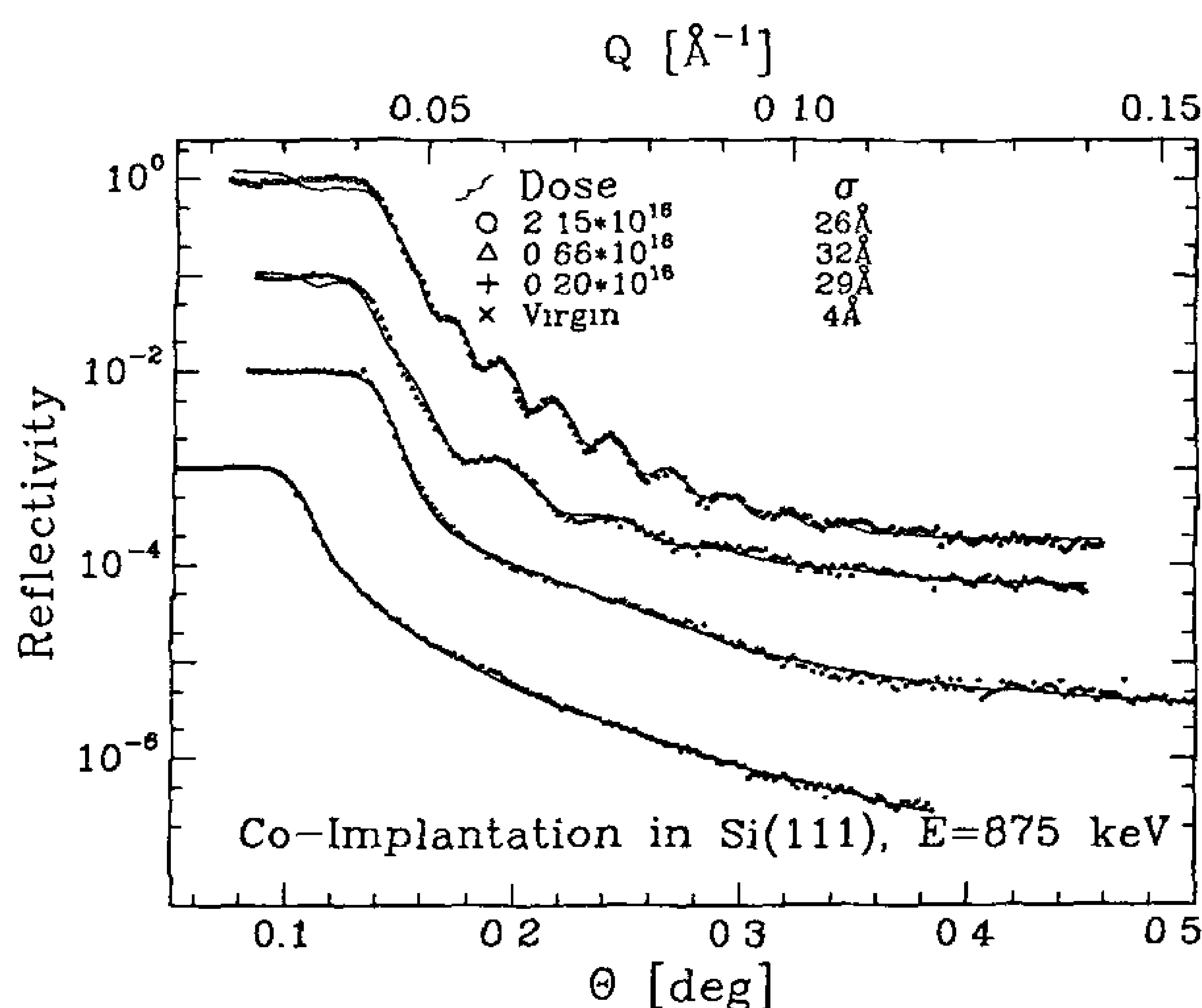

Figure 5 Reflectivity from Co-implanted Si(1 1 1) samples with various Co doses (ions/cm^2) and from a virgin Si(1 1 1) sample is shown The surface roughness values (σ) are listed The ordinates of the successive curves have been shifted by a decade for clarity.

Co^+ implantation was done at a tilt angle of 70°. The samples were not annealed. The reflectivity results are shown in Figure 5. A comparison with the virgin Si(1 1 1) sample shows that the surface roughness is significantly enhanced. However, the roughness is not strongly dose-dependent within the range of doses (2×10^{15}–2.15×10^{16} Co/cm^2) studied. The oscillations on the reflectivity curves arise from the interference due to scattering from a carbon layer deposited on the surface during implantation. The thickness of this layer is determined from the periodicity of these oscillations. Independently, we have determined the thickness of this carbon film and the depth distribution of Co atoms by Rutherford backscattering spectrometry[13]. Detailed analysis of the Co-implanted system will be published elsewhere.

X-ray reflectivity from a multilayer system has been worked out by Parrat[5]. For the multilayer system each interface can be represented by a Gaussian of the form given in eq. (6), with σ_l representing the rms roughness of the $(l-1)$th interface. (The first layer being vacuum, σ_2 represents the roughness of the surface of the second layer or the first interface.)

We believe that now with the availability of this powerful technique in India, further activities will be stimulated in the fast-developing area of surface and interface physics.

1 Dev, B N, Materlik, G, Grey, F, Johnson, R L. and Calusnitzer, M, *Phys. Rev Lett*, 1986, **57**, 3058–3061.
2 Vlieg, E, Fischer, A E M J, van der Veen, J F, Dev, B. N. and Materlik, G, *Surf Sci*, 1986, **178**, 36–46, Zegenhagen, J, Huang, K -G, Gibson, W M, Hunt, B D and Schowalter, L. J, *Phys Rev*, 1989, **B39**, 10254–10260
3. Fischer, A. E. M J., Vlieg, E., van der Veen, J F, Clausnitzer, M and Materlik, G., *Phys Rev*, 1987, **B36**, 4769–4773.
4 Satyam, P V. and Dev, B. N, *Indian J. Phys*, 1994, **A68**, 23–32.
5. Parrat, L. G., *Phys Rev*, 1954, **95**, 359–369
6. Satyam, P. V. and Dev, B N., *Indian J. Phys*, 1995, **A69**, 417–427.
7 James, R W, *The Optical Principles of the Diffraction of X-rays*, Ox Bow, Woodridge, 1982, Chap 13
8 Nevot, L and Croce, P, *Rev. Phys. Appl.*, 1980, **15**, 761.
9 Sinha, S K, Sirota, E. B., Garoff, S. and Stanley, H B, *Phys. Rev*, 1988, **B38**, 2297–2311.
10. Gog, Th, Harasimowicz, T., Dev, B. N. and Materlik, G., *Europhys Lett*, 1994, **25**, 253–258
11. Vanderstrten, H., Bruynseraede, Y., Vantomme, M F., Wu, A., Langouche, G. and Phillips, J. M, *Appl. Phys Lett.*, 1990, **57**, 135–137.
12. Gutzmann, A., Klaumuenzer, S. and Meier, P, *Phys. Rev. Lett.*, 1995, **74**, 2256–2259
13. Satyam, P V., Sundaravel, B, Ghose, S. K., Rout, B, Bahr, D. and Dev, B. N (to be published).

ACKNOWLEDGEMENTS Prof G. Materlik of Hamburg Synchrontron Radiation Laboratory (HASY-LAB at DESY) provided us the monochromator crystal and a slit system. The short visit of Dr D. Bahr from Prof. Materlik's group was supported by our Indo-German bilateral collaboration (Physics-25) We thank Prof. V. S. Ramamurthy for his support and encouragement.

Received 4 May 1995; revised accepted 20 July 1995

Single-ion activities by a solid ion transmitter bridge and a reference electrode without liquid junction

S. Parthasarathy and K. Ramya

Centre for Electrochemical and Energy Research, SPIC Science Foundation, 110, Mount Road, Madras 600 032, India

It had been shown that it is possible to measure thermodynamic values of single-ion activity using a solid ion conductor to bridge a reference electrode and a test electrode, thus eliminating liquid junction potentials. This led to redefinition of activity of an ion and brought out into sharp focus the crucial role of the charge factor in determining the effective strength of an ion. In this paper, we have measured potentials, free from liquid junction, using chloride ion sensors and the solid-ion transmitter bridge for determining chloride ion activity in zinc chloride solutions, leading to confirmation of definition of activity of an ion already proposed.

THE central paradigm of the theory of ionic solutions of strong electrolytes can be stated as follows:

1. It is impossible to measure the activity of single ion in solutions of strong electrolytes, as any reference